GEOPHYSICAL RESEARCH LETTERS, VOL. 25, NO.24, PAGES 4441-4444, DECEMBER 15, 1998

Multi-fluid simulations of the magnetosphere: The identification of the geopause and its variation with IMF

R. M. Winglee

Geophysics Program, University of Washington, Seattle WA 98195-1650

Abstract. A new multi-fluid global treatment is presented that separately tracks the solar wind and ionospheric plasmas in the magnetosphere. The model is used to identify the density and pressure geopauses, i.e. the boundaries where the contributions to the magnetospheric density or pressure from the ionosphere equals that from the solar wind. The density geopause is primarily restricted to the inner magnetosphere and central lobes for northward interplanetary magnetic field (IMF) but during southward IMF it can extend into middle magnetosphere due to enhanced ionospheric outflow and convection. This variation is consistent with recent statistical studies that show that the plasma sheet density is correlated with the solar wind density, particularly during northward IMF.

Introduction

In the late 1980's results from S3-3 and Dynamics Explorer 1 showed that there was substantial heating of ionospheric plasma and that this plasma was able to flow out into the magnetosphere. These observations lead to the suggestion that the ionosphere can be an important source of plasma to the magnetosphere [*Moore et al.*, 1986; *Chappell et al.*, 1987]. *Moore* [1991] and *Moore and Delcourt* [1995] extented the concept further by proposing that within the magnetosphere there was a boundary called the geopause, where the dynamics within this boundary was dominated by ionospheric plasma, and regions outside by plasma of solar wind origin. The geopause was envisaged to extend into at least the mid-tail region as suggested by single particle tracking [*Delcourt et al.*, 1989, 1993].

On the other hand, very strong mass loading of the magnetosphere by solar wind plasma has been documented in recent statistical studies where the tail density appears to be well correlated with the solar wind density. Such correlations have been seen both by Geotail [*Terasawa et al.*, 1997] and by ISEE [*Borovsky et al.*, 1997]. In both cases the mass loading appears to be strongest for northward IMF when the magnetosphere paradoxically is expected to be relatively closed.

In order to understand the origins of the different plasma populations within the magnetosphere, a new multi-fluid treatment of the magnetosphere is presented. Unlike MHD which is a single fluid treatment, the new method is able to distinguish the ionospheric populations from the solar wind populations, and provides the first 3-D visualization of the geopause as a function of the solar wind conditions.

Paper number 1998GL900217.
0094-8276/98/1998GL900217$05.00

Multi-Fluid Simulations

The fluid description of a plasma is given by

$$\frac{\partial \rho_\alpha}{\partial t} + \nabla \cdot (\rho_\alpha \boldsymbol{V}_\alpha) = 0 \tag{1}$$

$$\rho_\alpha \frac{d\boldsymbol{V}_\alpha}{dt} = q_\alpha n_\alpha (\boldsymbol{E} + \frac{\boldsymbol{V}_\alpha \times \boldsymbol{B}}{c}) - \nabla P_\alpha \tag{2}$$

$$\frac{\partial P_\alpha}{\partial t} = -\gamma \nabla \cdot \left(P_\alpha \boldsymbol{V}_\alpha\right) + (\gamma - 1)\, \boldsymbol{V}_\alpha \cdot \nabla P_\alpha \tag{3}$$

where γ is the polytropic index. MHD sums the above equations to attain a tractable solution with a single temperature, density and bulk velocity.

The global multi-fluid treatment presented here is not limited by such restrictions, and instead provides separate tracking of the electrons and the dominant ion species. For the electrons, they are assumed to have high mobility along the field lines so that they are approximately in steady state or drift motion, i.e,

$$\boldsymbol{E} + \frac{\boldsymbol{V}_e \times \boldsymbol{B}}{\boldsymbol{c}} + \frac{\nabla P_e}{e n_e} = 0 \tag{4}$$

The rest of the electron dynamics is given by assuming quasi-neutrality, and applying the definitions for current, and electron pressure, i.e.,

$$n_e = \sum_i n_i, \;\; \boldsymbol{V}_e = \sum_i \frac{n_i}{n_e} \boldsymbol{V}_i - \frac{\boldsymbol{J}}{e n_e}, \;\; \boldsymbol{J} = \frac{c}{4\pi} \nabla \times \boldsymbol{B} \tag{5}$$

$$\frac{\partial P_e}{\partial t} = -\gamma \nabla \cdot (P_e \boldsymbol{V}_e) + (\gamma - 1)\, \boldsymbol{V}_e \cdot \nabla P_e \tag{6}$$

The ion dynamics is attained by substituting the modified Ohm's law (4) for the electric field in the ion momentum equation, which gives

$$\rho_\alpha \frac{dV_{\parallel\alpha}}{dt} = -(\nabla P_\alpha)_\parallel - \frac{n_\alpha}{n_e} (\nabla P_e)_\parallel \tag{7}$$

$$\rho_\alpha \frac{dV_{\perp\alpha}}{dt} = e n_\alpha \Big(\frac{V_\alpha \times B}{c} - \sum_i \frac{n_i}{n_e} \frac{V_i \times B}{c}\Big) + \frac{n_\alpha}{n_e} \Big(\frac{J \times B}{c} - (\nabla P_e)_\perp\Big) - (\nabla P_\alpha)_\perp \tag{8}$$

where the $\parallel$ and $\perp$ subscripts indicate components parallel and perpendicular to the magnetic field, respectively. For

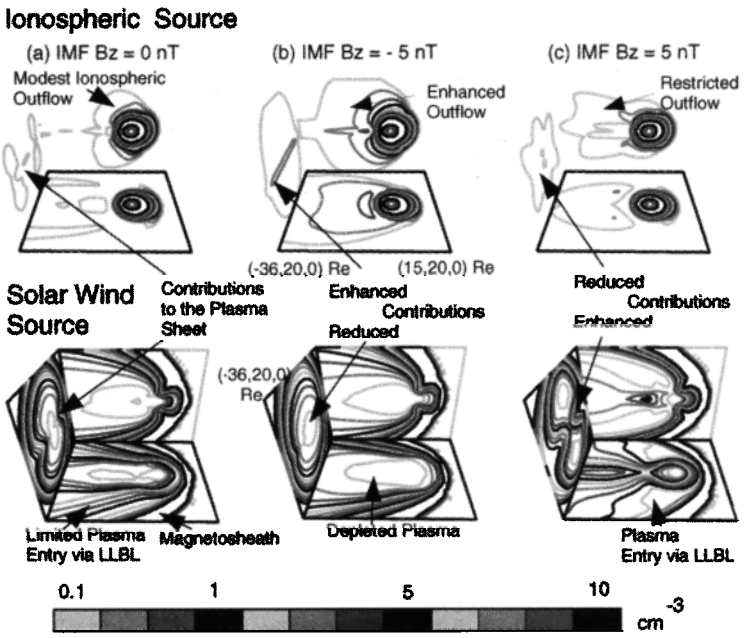

Figure 1. The densities of the ionospheric source (top panels) and the solar wind source (lower panels) for IMF B_z equal to (a) zero, (b) -5 nT, and (c) 5 nT. The noon-midnight meridian is shown in the back, the equatorial plane at the bottom, and the side contours the densities at $x = -15\ R_E$.

a plasma with a single ion component, (9) reduces to the MHD momentum equation.

To remove high-frequency cyclotron oscillations, the different ion species are assumed to have the same drifts across the field line, i.e.,

$$\boldsymbol{V}_\perp = \sum_i \rho_i \boldsymbol{V}_{i,\perp} / \sum_i \rho_i \ . \qquad (9)$$

This approximation is the same as in MHD, and assumes that the convective drifts are much larger than the gradient B drifts. For the calculated bulk temperatures (< 10 keV), this assumption is true for the bulk of the plasma, but the particles in the tail of the distribution can have significant gradient B drifts.

The above equations are solved using a two-step Lax-Wendroff differencing scheme [*Richtmyer and Morton*, 1967] with a flux-correction transport scheme [*Boris and Book*, 1973] applied to plasma properties only. The corrections removes unphysical grid point oscillations across sharp discontinuities such as the bow shock. A grid resolution of 0.4 R_E is used in the near Earth region from +15 to - 30 R_E in x and ±15 R_E in y and z in the geocentric solar magnetic (GSM) system. The grid spacing then increases, being about 3 R_E in the distant tail at $x \simeq 200 R_e$ and at the flanks at $\pm 60 R_E$.

A constant solar wind density at 6 cm^{-3} and a speed of 400 km/s are assumed. The simulations are first run for 2-hrs real time to attain an approximate equilibrium for the magnetosphere. In order to show that the results are not dominated by numerical diffusion but are ordered by IMF B_z, we consider sequentially three 1-hr periods with: (a) B_z ramped between ±1.25 nT, (b) B_z = -5 nT, and (c) B_z = +5 nT.

The inner radius of the simulations is 2.5 R_E. A plasma with a density of 400 cm^{-3} and which falls off as R^{-6} is placed around the inner radius, representing the plasmaspheric/ionospheric source [e.g. *Parks*, 1991]. The solar wind and ionospheric plasmas are assumed to be H^+ but they can be differentiated through their distinct energy characteristics.

The initial plasma temperature in the equatorial region is assumed to decrease as R^{-3}. The initial pressure along each flux tube is assumed constant (by setting the pressure at each grid point to that of the field line mapped to the equator). The equatorial bulk temperature is set to about 60 eV and in the polar cap it is less that 0.3 eV. The high temperature at the equator allows for the presence of some ring current/plasma sheet population for an energy density of 20 keV/cc [cf. *Parks*, 1991]. The low temperature in the polar cap region is within the observed range and limits thermal outflow of ionospheric plasma. The total ion outflow seen in the simulations is about 6×10^{26} ions/s for the northward IMF case increasing to 2×10^{27} ions/s for the southward IMF. These numbers are order of those estimated by *Chappell et al.* [1987].

Relative Density for Varying IMF

Figure 1 shows contours of the densities in the near-Earth region derived for the 3 IMF cases. For the zero IMF case, most of the ionospheric plasma is restricted to the inner magnetosphere forming a plasmasphere. The main contributions from the ionospheric source to the tail are (1) convected flows out of the polar regions that produce weak contributions to the tail current sheet in the mid-tail region and (2) convection of dayside plasma towards the magnetopause where it is subsequently convected along the flanks to make the weak contributions to the low latitude boundary layer (LLBL).

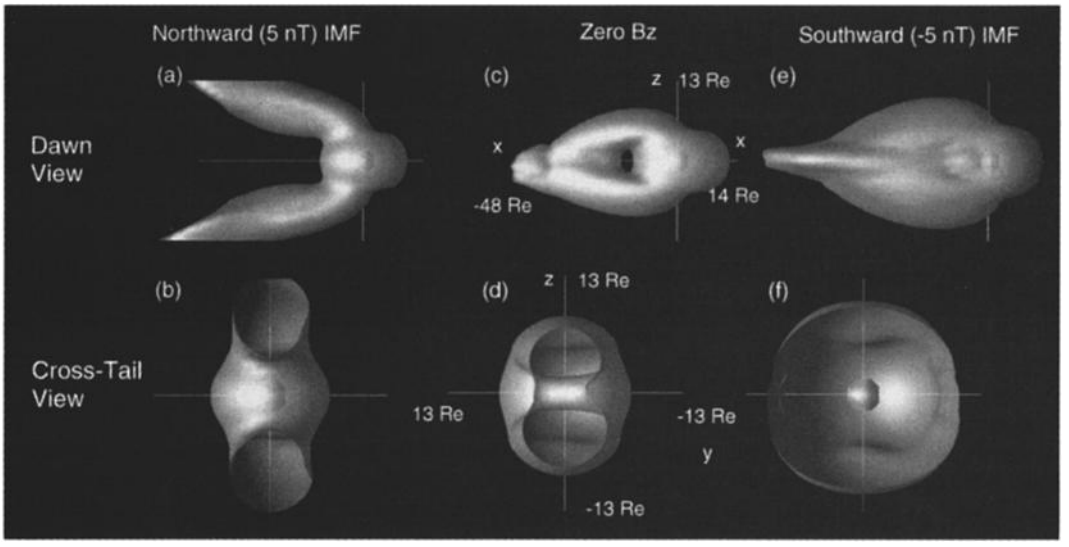

Figure 2. The density geopauses corresponding to Figure 1, except the ordering is by B_z IMF rather than by time. The top panels show views from the dawn side while the bottom shows views from the nightside with the surface being cut at $x = -15\ R_E$.

In contrast, the plasma of solar wind or magnetosheath origin shows much greater penetration into the LLBL and provides much of the density for the plasma sheet. The magnetosheath entry is via high-latitude reconnection during northward IMF where field lines loaded with solar wind plasma become attached to the dayside magnetosphere. The subsequent convection of these reconnected field lines into the nightside leads to the high densities at the LLBL and plasma sheet. The presence of a small negative B_x IMF causes a fractional enhancement in the southern hemispheric densities relative to the northern hemisphere.

During southward IMF (Figure 1b), there is enhanced convection of ionospheric plasma out of the polar caps regions. As a result, the density in the lobes is substantially increased, leading to an enhanced ionospheric contribution to the plasma sheet. In addition, dayside plasmaspheric plasma is increasingly convected towards the magnetopause, then around the flanks along the LLBL, and into the nightside to produce an equatorial bulge in the plasma sheet contributions.

At the same time the magnetosheath plasma is seen to become substantially depleted in density, particularly in the center of the current sheet, while there is increased penetration into the lobes. This change in the contributions arises from the suppression of high latitude reconnection and entry into the LLBL. Entry into the magnetosphere via the mantle is possible but the plasma has limited access to the plasma sheet.

When the IMF is strongly northward (Figure 1c), the ionospheric outflows are strongly suppressed due to the reduction in cross-polar cap potential. The refilling of the magnetosphere is again via magnetosheath entry through the LLBL.

The question of which of the two plasma sources actually dominates the dynamics can be answered by considering the geopause. The density geopauses for the cases in Figure 1 are shown in Figure 2, with the ionospheric source being the primary contributor to the plasma inside the surface, and the solar wind plasma the dominant contributor outside the surface. The ordering has been changed to show that IMF B_z provides a natural ordering of the results.

For northward IMF the ionospheric source is the primary contributor to the plasmasphere and to the central lobe regions. While the ionospheric contributions to the lobe plasma can extend several tens of R_E down the tail, its is highly restricted in extent being limited to between $y \simeq \pm 4\ R_E$. The plasma sheet for these conditions is dominated by the solar wind source.

As IMF B_z is reduced to zero (Figures 2c and 2d), the corresponding enhancement in the convection of ionospheric plasma into the magnetosphere is seen as (1) an extension of the plasma on the dayside, (2) a broadening of the contributions to the lobe, and (3) convection of this plasma into the plasma sheet so that the ionospheric source can be the dominant contribution to the plasma sheet between 10 and 50 R_E in a restricted region across the tail for $y \simeq \pm 5\ R_E$.

For strongly southward IMF (Figures 2e and 2f), the influence of the ionospheric source is seen to further expand in y across the tail to about $\pm 10\ R_E$ which represents about a third to a half of the distance to the nightside magnetopause. At the same time, the geopause moves down the tail to about 65 R_E. These results show that for at least some of the time, particularly for southward IMF, the ionospheric source can be an important contributor to not only the lobe plasma but also to the plasma sheet.

There is a second geopause, the pressure geopause (Figure 3), which is crucial to understanding which of the two populations supplies hot plasma that provides pressure balance. It can extend much further down the tail. This difference between the density and pressure geopauses is very important. The region inside the density geopause but outside the pressure geopause indicates regions where the ionospheric source is primarily supplying cold plasma. This region in the present cases primarily corresponds to the lobe regions. Conversely, if the region is outside the density geopause, but inside the pressure geopause, then the ionospheric source is primarily supplying the hot plasma. In Figure 3 this region appears as the central current sheet in

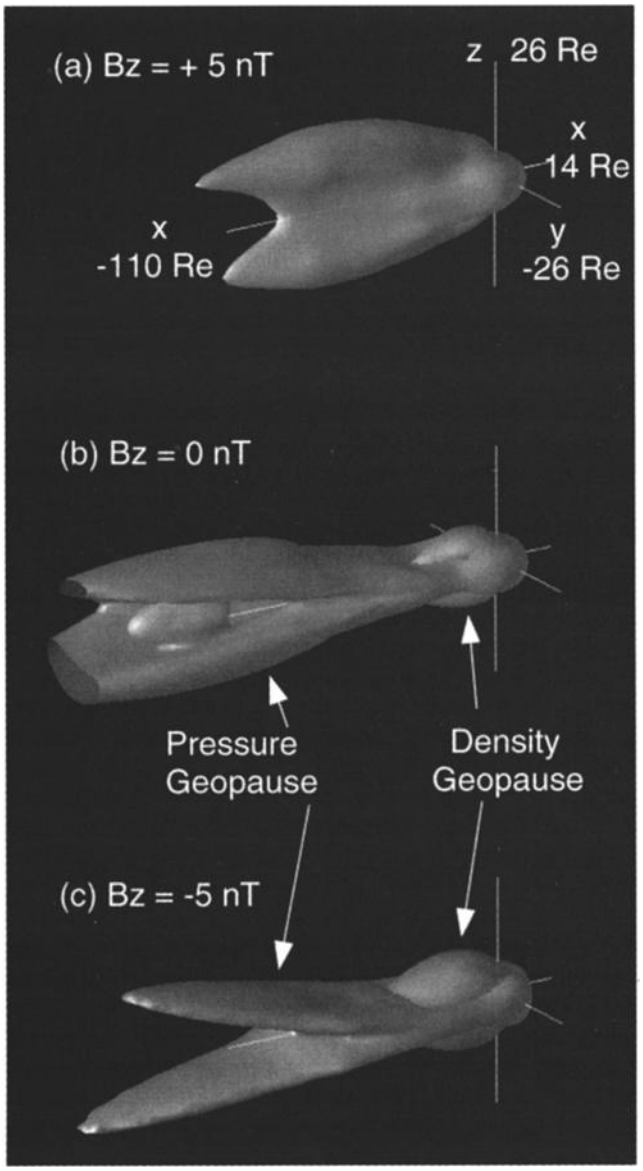

Figure 3. The pressure geopause superposed over the density geopause for the three cases in Figure 2. The pressure geopause extends deeper into the tail and indicates that much of the hot plasma in the tail is from the ionospheric source.

the middle to inner magnetosphere and to the plasma sheet boundary layer in the distant tail.

The reason that the ionospheric plasma appears to be preferentially heated is that it has access to much stronger current sheet acceleration that the solar wind source. The density geopause in Figure 2 indicates that the ionospheric source has the greater access to the region between 10 and 40 R_E down the tail, particularly along the noon-midnight meridian, and it is this region where the near-Earth neutral line forms. It is for this reason that in the distant tail the pressure geopause has the form of two tubes in a "V" formation (Figures 3b and 3c) as the ionospheric plasma jets out of the near-Earth neutral line. Because of the absence of the neutral line during northward IMF, the pressure geopause is seen to pinch, in particularly around the equator (Figure 3a).

Summary

A multi-fluid global model of the magnetosphere has been used for the first time to examine the dynamics of the magnetosphere for idealized solar wind conditions. The simulations show that the ionosphere can be an important source of plasma in the nightside, particularly during southward IMF due to enhanced convection of plasma out of the auroral and polar cap regions. This ionospheric plasma can reach the region where the near-Earth neutral line tends to form. As a result, it is the ionospheric source that provides much of the hot plasma seen in the current sheet.

The relative contributions to the magnetosphere from the ionospheric and solar wind sources are best visualized through the density and pressure geopauses. The density geopause is more closely confined to the inner magnetosphere for northward IMF where high-latitude reconnection and subsequent convection of the reconnected field lines allows the solar wind source to provide most of the plasma in the tail. This result provides a simple explanation for the apparent correlation between the solar wind density and the plasma sheet density, particularly during northward IMF [*Terasawa et al.*, 1997; *Borovsky et al.*, 1997].

Acknowledgment. This work was supported by NSF Grant ATM-9731951 and by NASA grant NAGW-5047 to the Univ. of Washington. The simulations were supported by the Cray T-90 at the San Diego Supercomputing Center which is supported by NSF.

References

Boris, J. A., and D. L. Book, Flux-corrected transport. 1. SHASTA, a fluid transport algorithm that works, *J. Computational Phys., 11*, 38, 1973.

Borovsky, J. E., M. F. Thomsen, and D. J. McComas, The superdense plasma sheet: plasmaspheric origin, solar wind origin, or ionospheric origin? *J. Geophys. Res., 97*, 22,089, 1997.

Chappell, C. R., T. E. Moore, and J. H. Waite, Jr., The ionosphere as a fully adequate source of the earth's magnetosphere, *J. Geophys. Res., 92*, 5896, 1987.

Delcourt, D. C, C. R. Chappell, T. E. Moore, and J. H. Waite, Jr., A three-dimensional numerical model of ionospheric plasma in the magnetosphere, *J. Geophys. Res., 94*, 11,893, 1989.

Delcourt, D. C, J. A. Sauvaud, and T. E. Moore, Polar wind ion dynamics in the magnetotail, *J. Geophys. Res., 98*, 9155, 1993.

Moore, T. E., et al., Upwelling O^+ source characteristics, *J. Geophys. Res., 91*, 7019, 1986.

Moore, T. E., Origins of magnetospheric plasma, *Rev. Geophys., 29*, 1039, 1991.

Moore, T. E., and D. C. Delcourt, 'The Geopause', *Rev. Geophys., 33*, 175, 1995.

Parks, G. K, *Physics of Space Plasmas* Addison-Wesley, Redwood City, California, 1991.

Richtmyer, R. D., and K. W. Morton, *Difference Methods for Initial Value Problems*, p. 300, Interscience, New York, 1967.

Terasawa, T., *et al.*, Solar wind control of density and temperature in the near-Earth plasma sheet: WIND/GEOTAIL collaboration, *Geophys. Res. Lett., 24*, 935, 1997.

Winglee, R. M., S. Kokubun, R. P. Lin, and R. P. Lepping, Flux rope structures in the magnetotail: Comparison between Wind/Geotail observations and global simulations, *J. Geophys. Res., 103*, 135, 1998.

R. M. Winglee, Geophysics Program, Box 351650, University of Washington, Seattle WA 98195-1650. (e-mail: winglee@geophys.washington.edu)

(Received July 13, 1998; revised October 19, 1998; accepted October 29, 1998.)